

SUPPLEMENTARY MATERIAL accompanying “Seasonal Trends in the Wintertime Photochemical Regime of the Uinta Basin, Utah” by Marc L. Mansfield and Seth N. Lyman

Figures S1 through S24 are ozone isopleth diagrams, one each for each of the 24 F0AM models described in the main text. The base case for each model is indicated by the symbol \otimes . Green squares indicate points at which NO_x sensitivity is zero, i.e., above them, ozone concentrations increase when NO_x concentration decreases. Blue squares indicate points at which NO_x and VOC sensitivity are equal. Below the blue squares, greater reductions in ozone can be achieved by reducing NO_x than by reducing VOC.

Figures S25 and S26 show correlations between $[\text{CH}_4]$, $[\text{NO}_x]$, and the pseudo-lapse rate Ψ .

D13a 2013-12-16

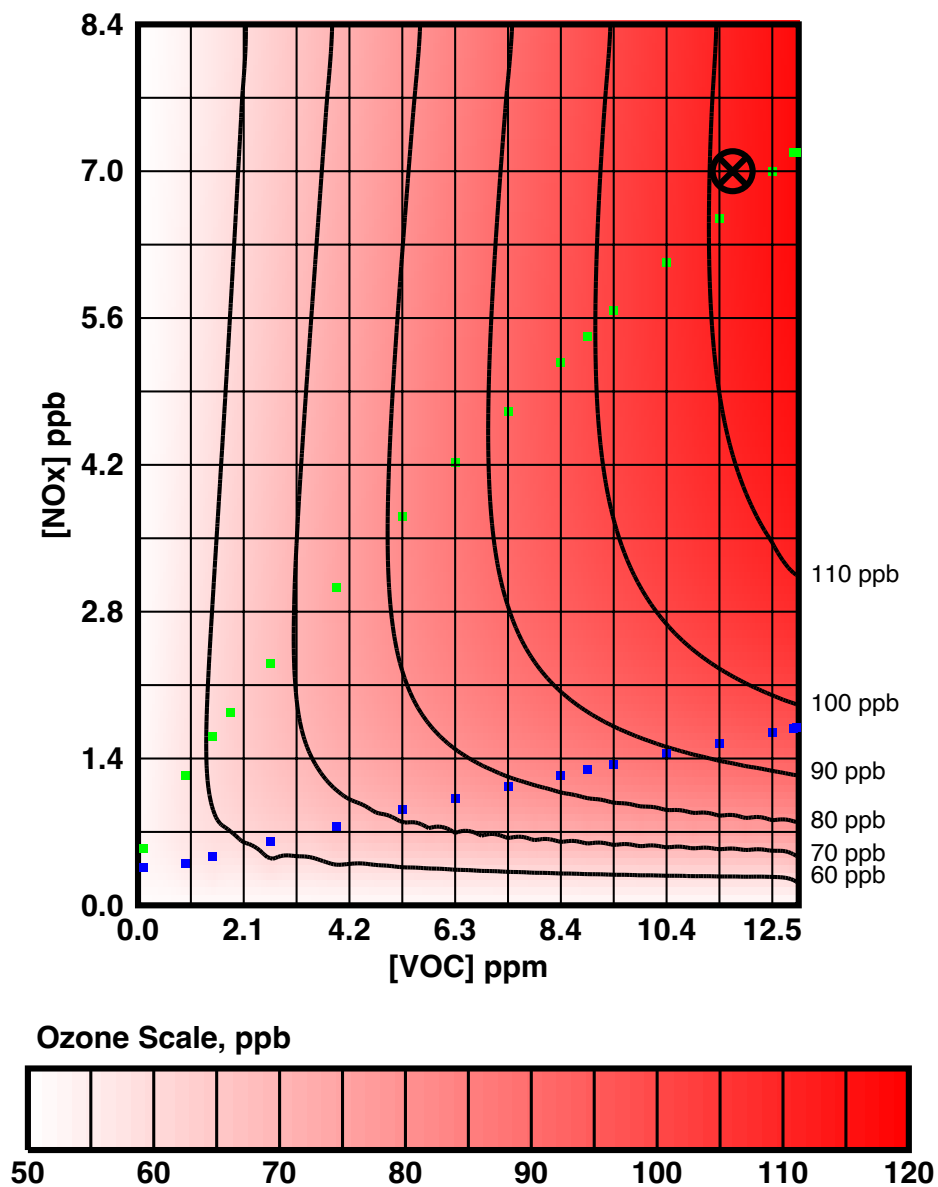


Figure S1. Model D13a, 2013-12-18.

D20a 2020-12-21

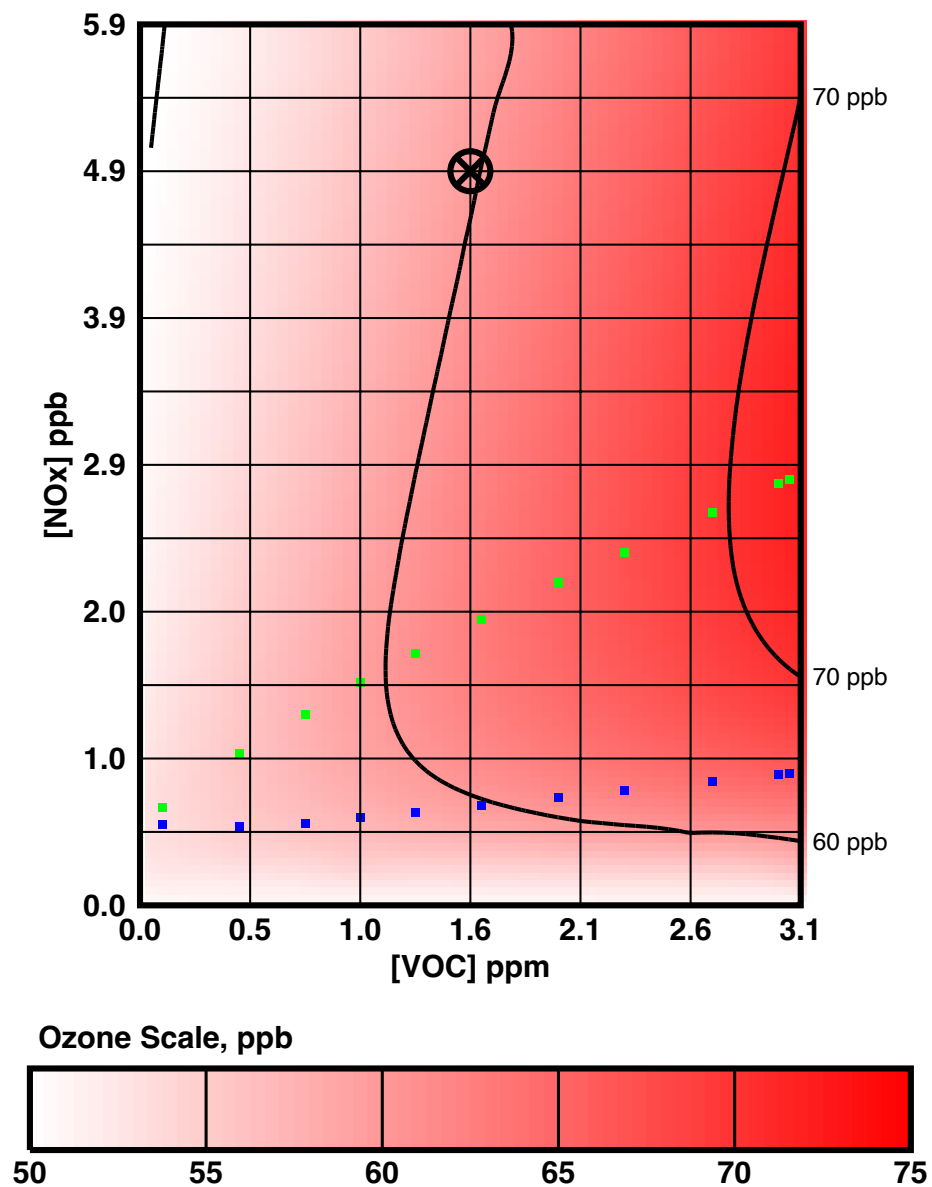


Figure S2. Model D20a, 2020-12-21.

D13b 2013-12-30

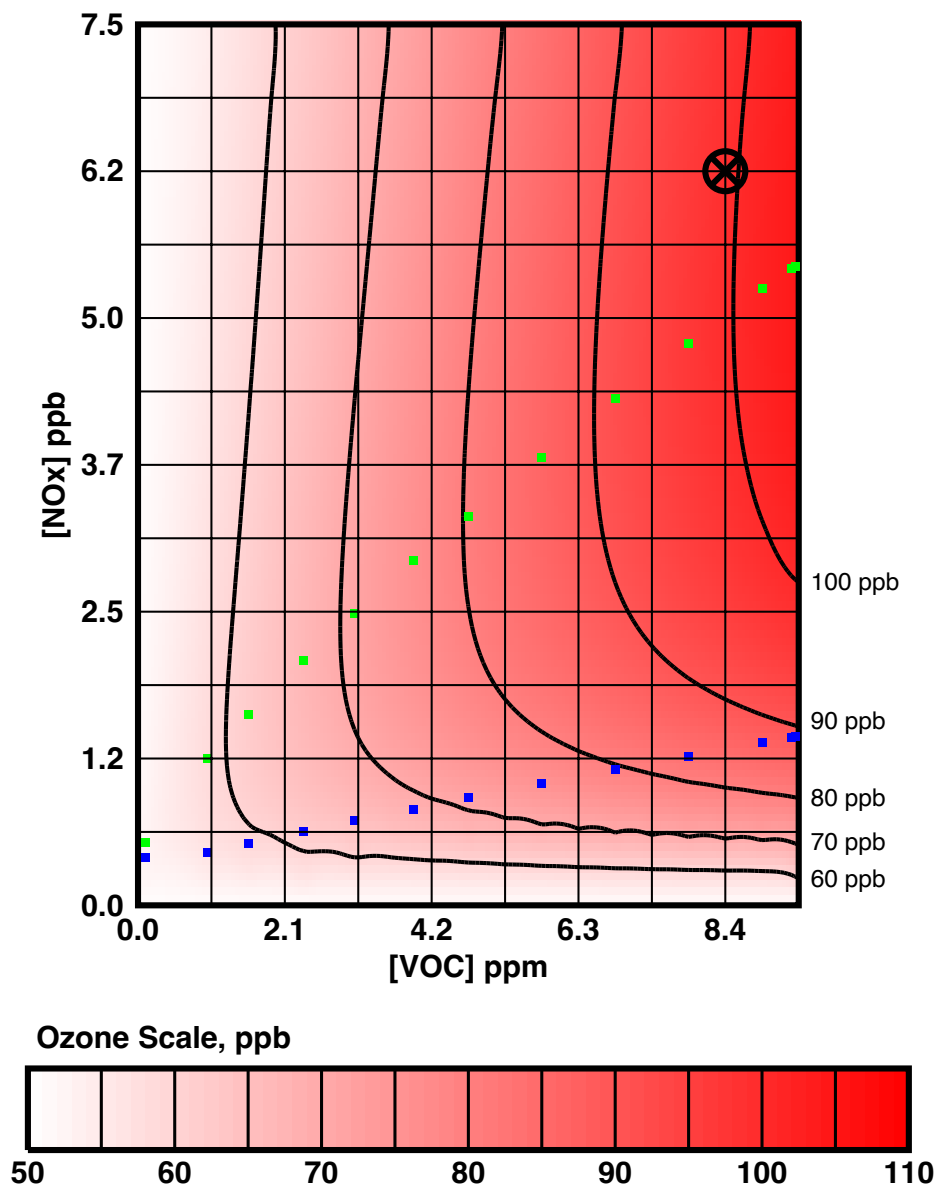


Figure S3. Model D13b, 2013-12-30.

J21a 2021-01-05

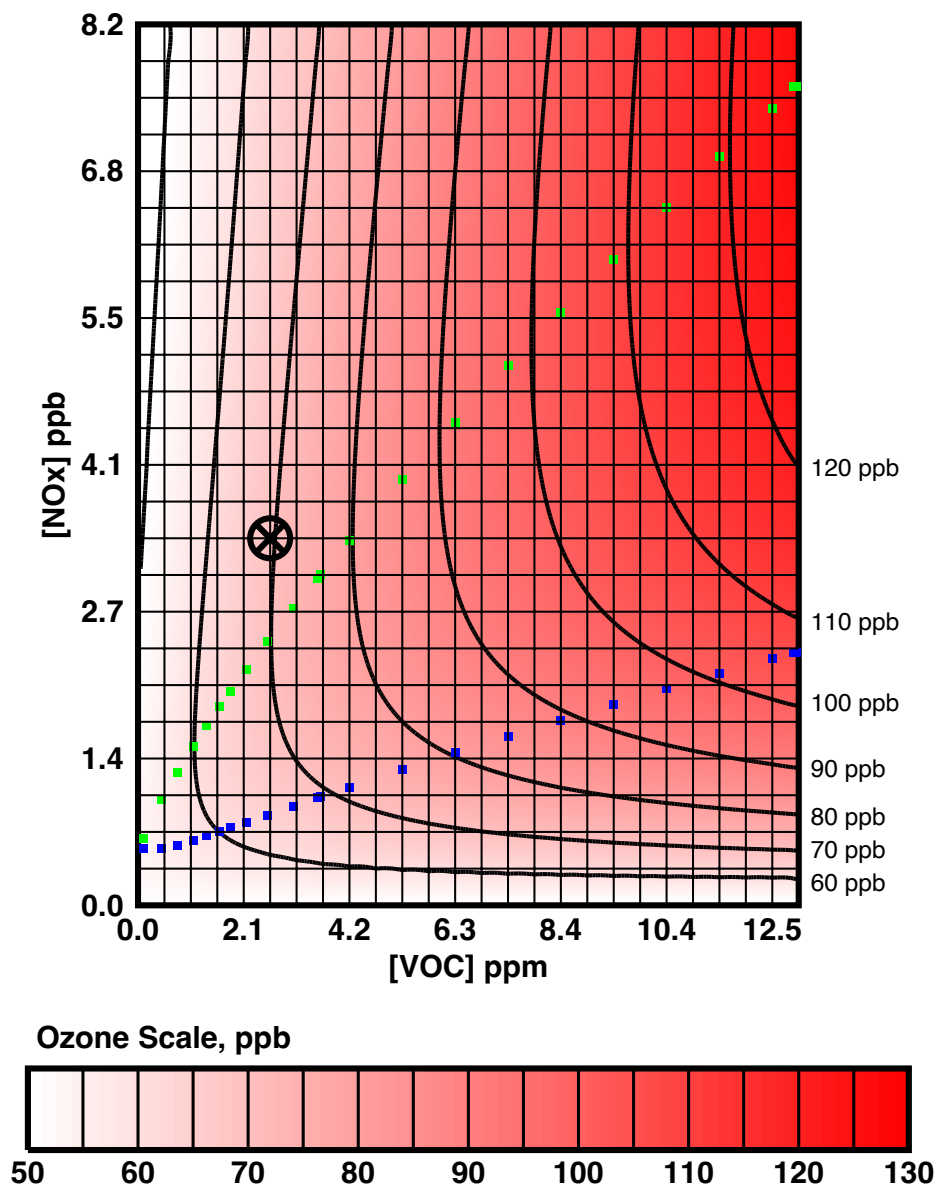


Figure S4. Model J21a, 2021-01-05.

J15a 2015-01-07

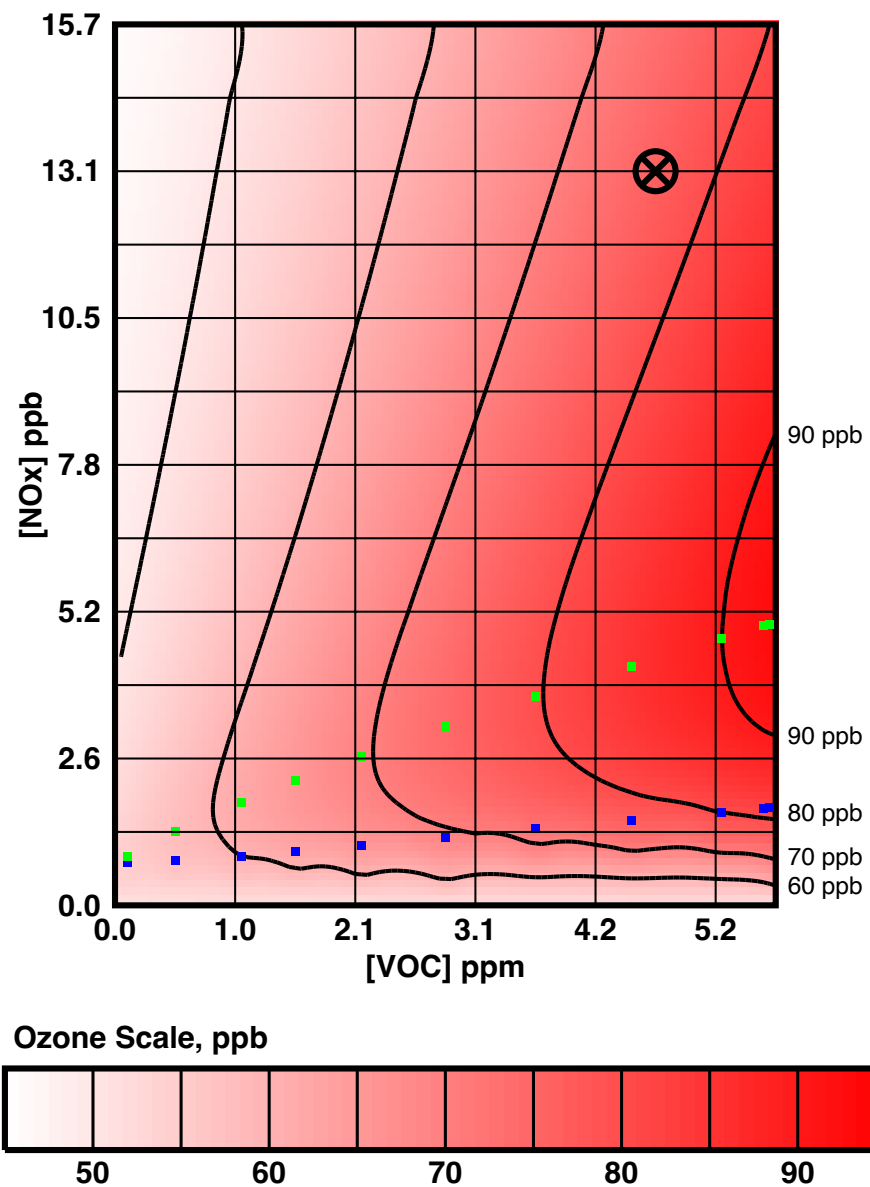


Figure S5. Model J15a, 2015-01-07.

J20a 2020-01-08

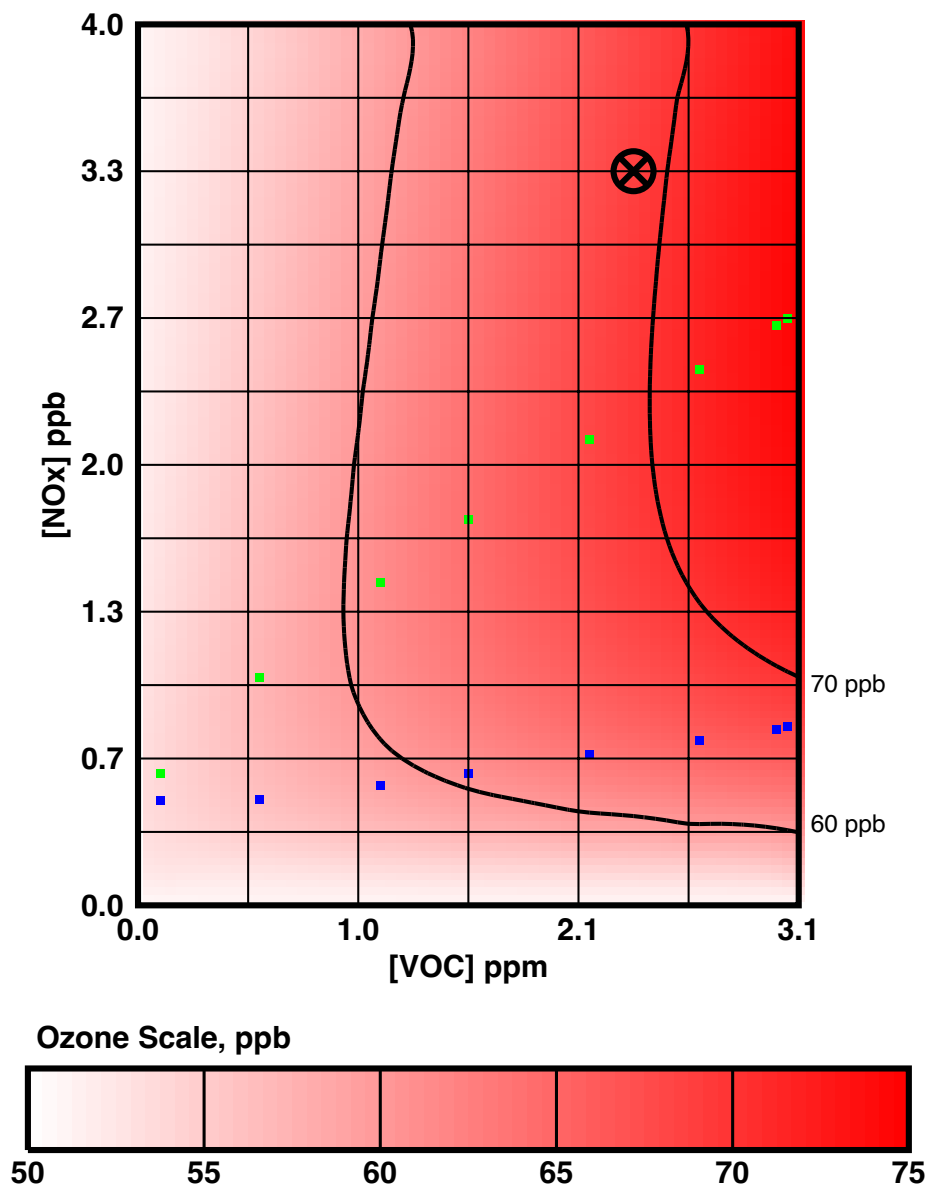


Figure S6. Model J20a, 2020-01-08.

J13a 2013-01-10

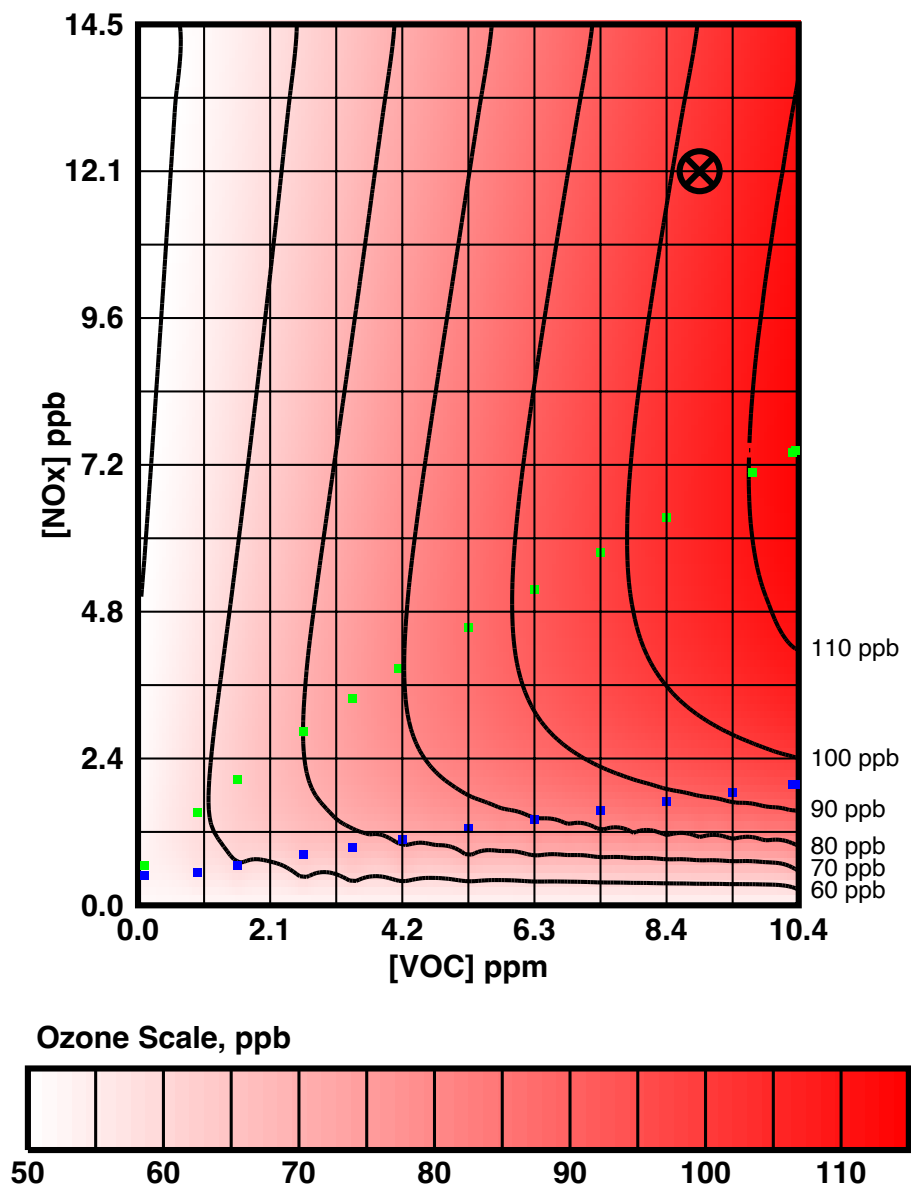


Figure S7. Model J13a, 2013-01-10.

J16a 2016-01-17

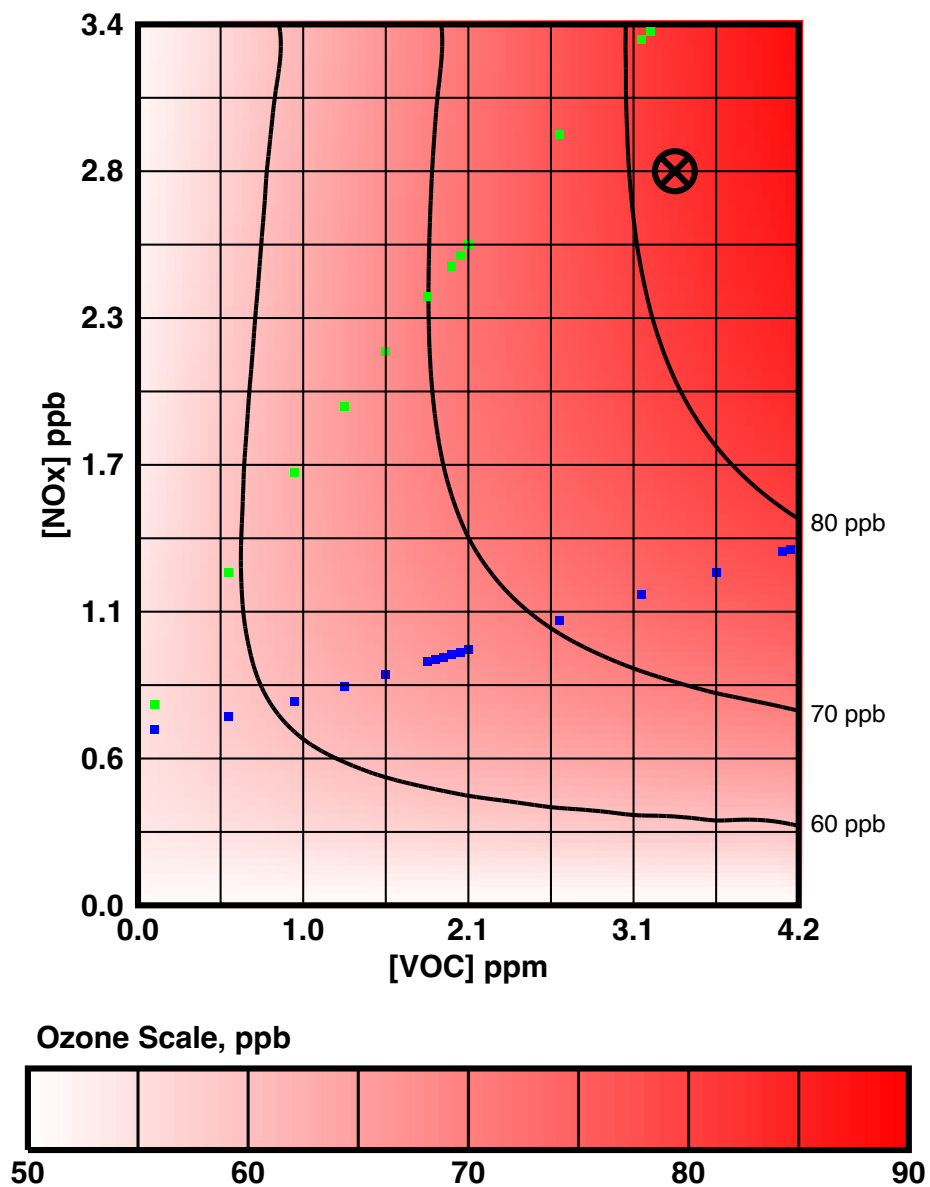


Figure S8. Model J16a, 2016-01-17.

J21b 2021-01-17

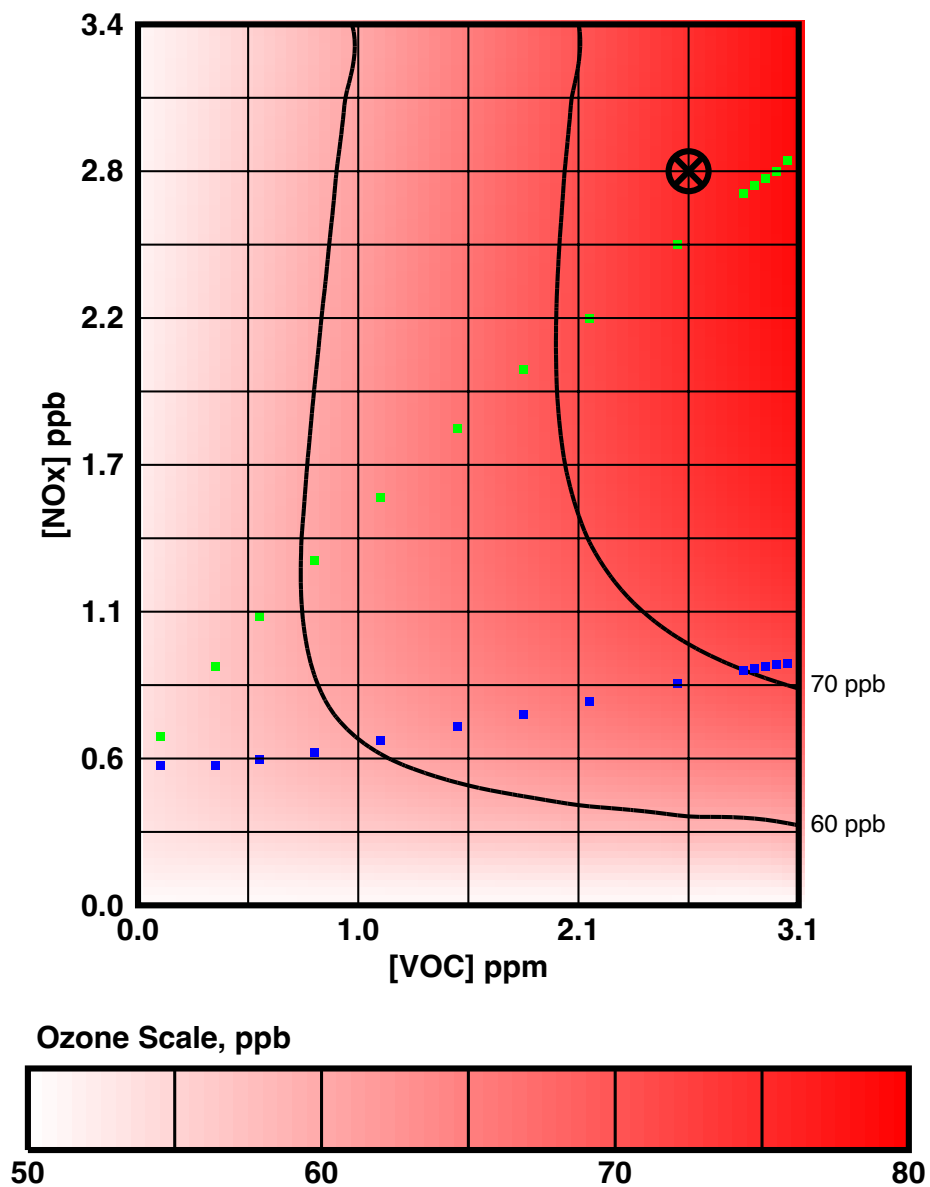


Figure S9. Model J21b, 2021-01-17.

J13b 2013-01-26

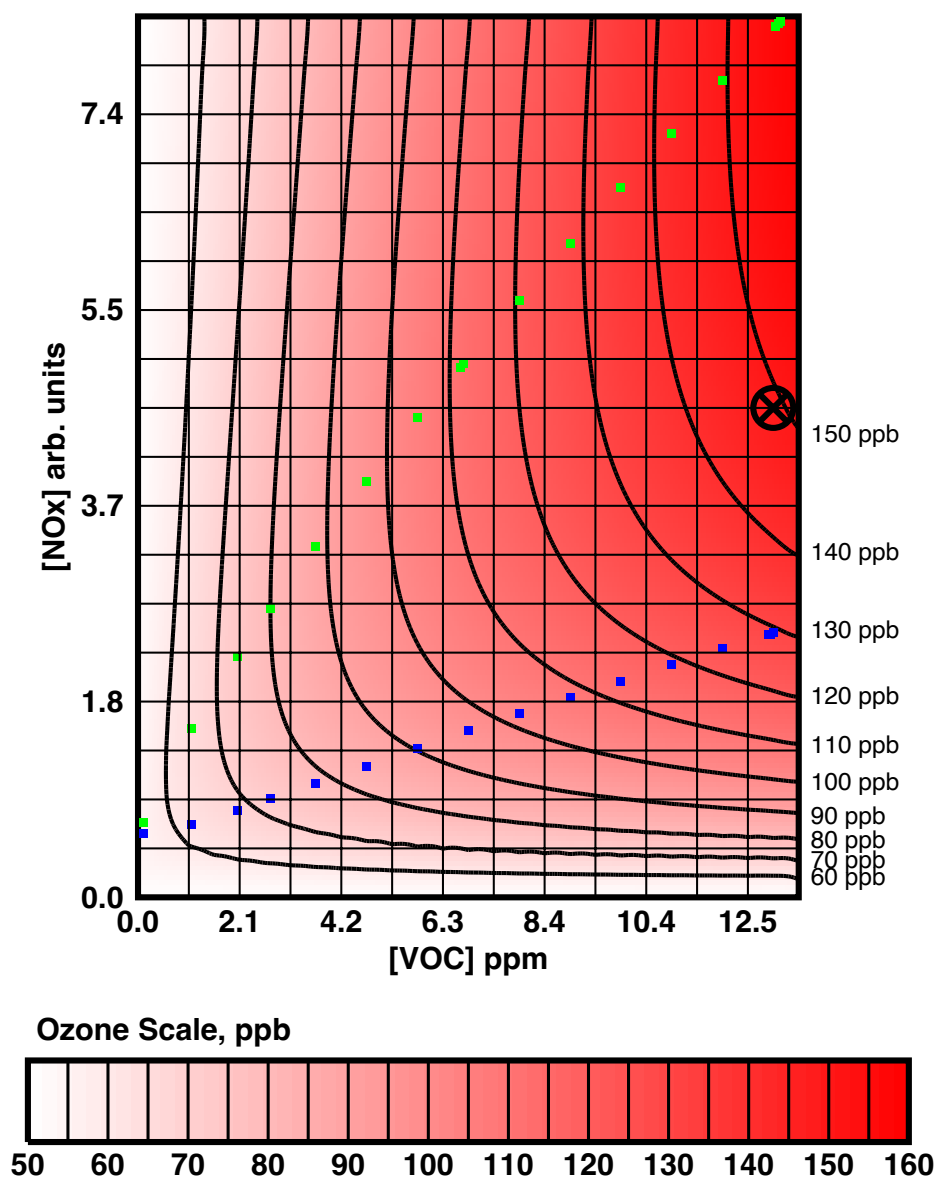


Figure S10. Model J13b, 2013-01-26.

J14a 2014-01-27

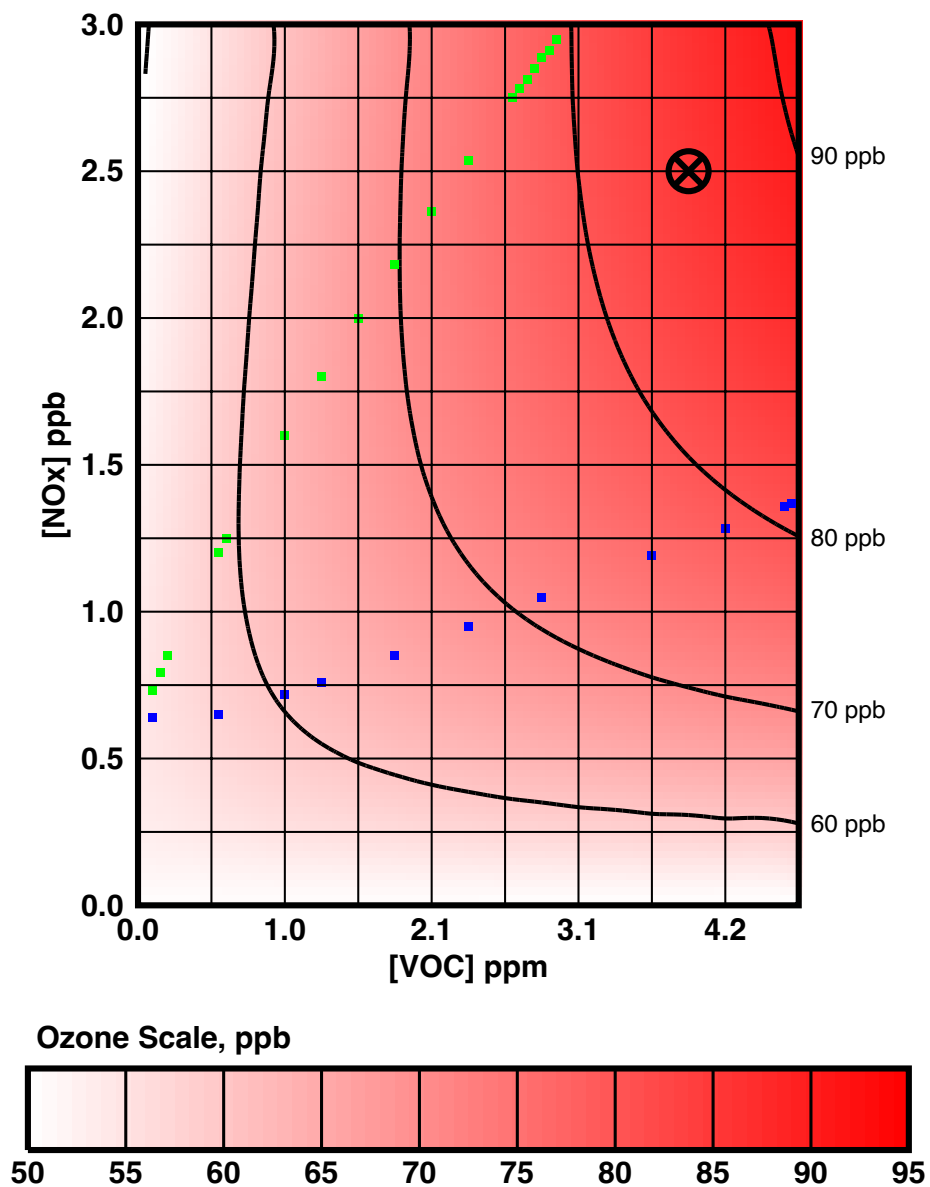


Figure S11. Model J14a, 2014-01-27.

J16b 2016-01-29

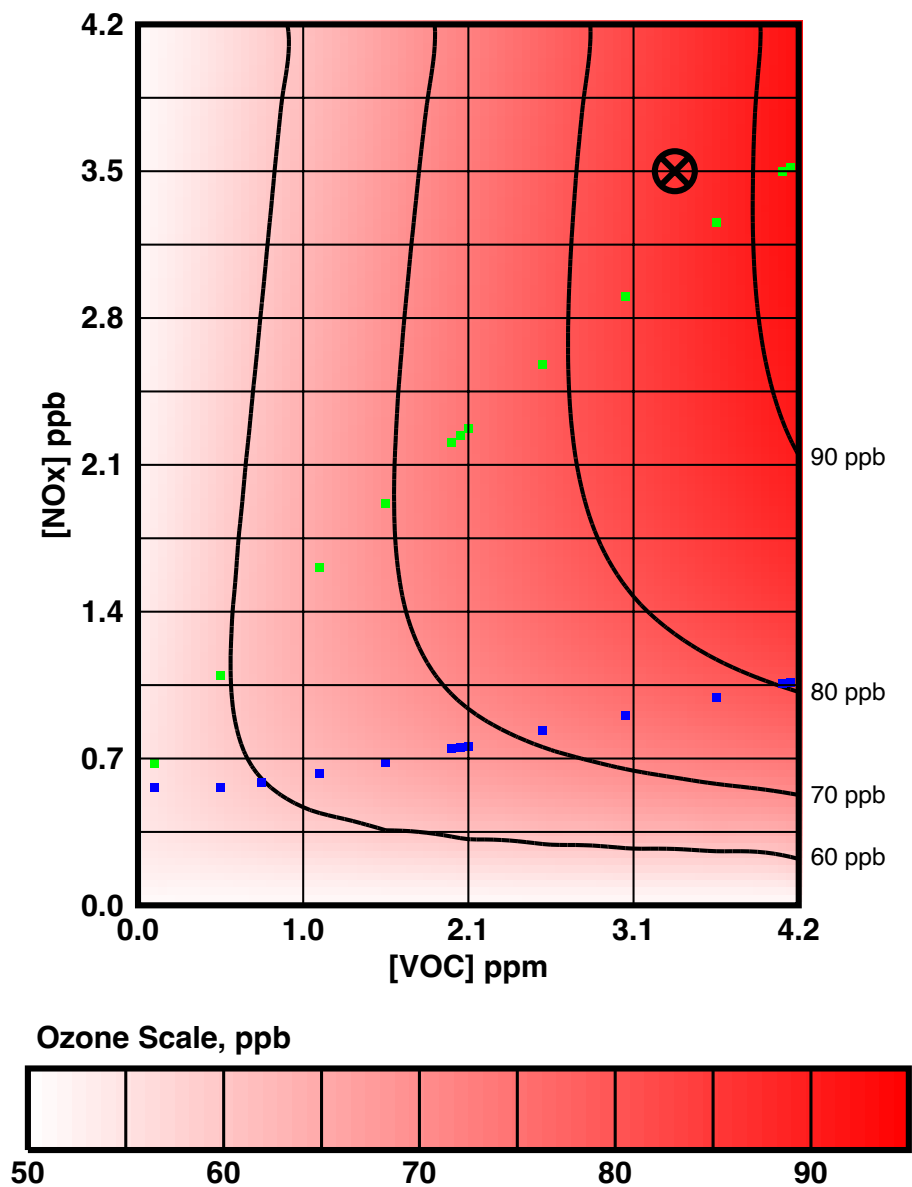


Figure S12. Model J16b, 2016-01-29.

F19a 2019-02-01

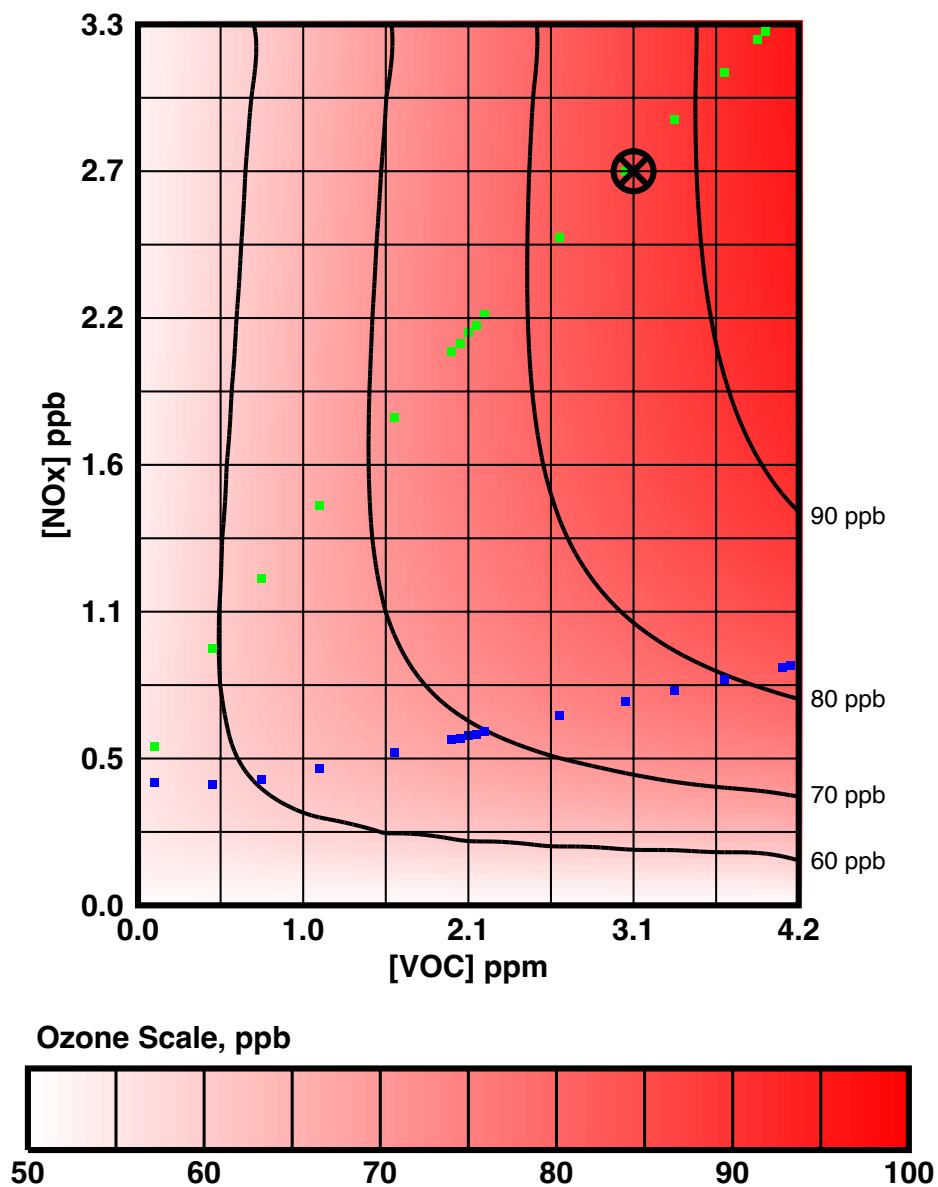


Figure S13. Model F19a, 2019-02-01.

F13a 2013-02-06

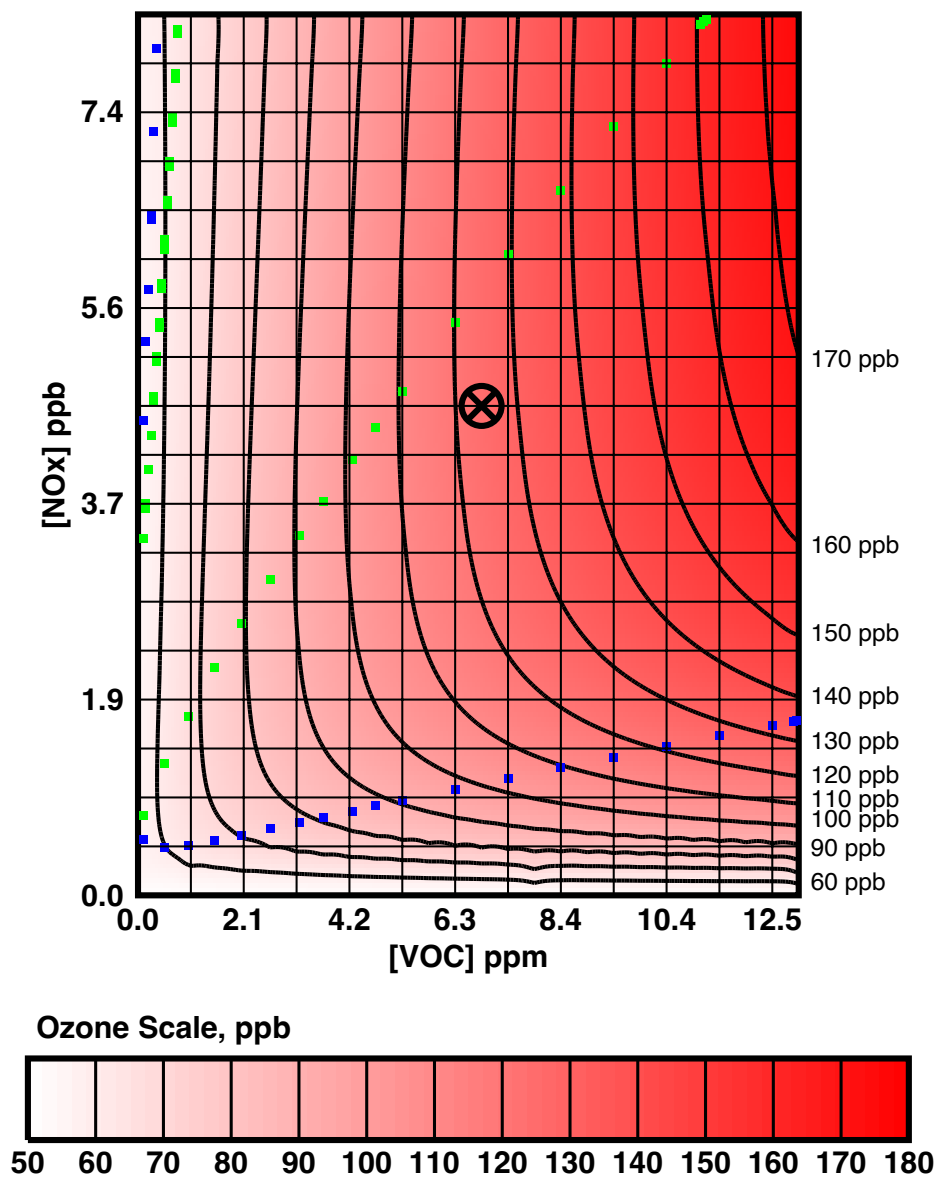


Figure S14. Model F13a, 2013-02-06.

F17a 2017-02-06

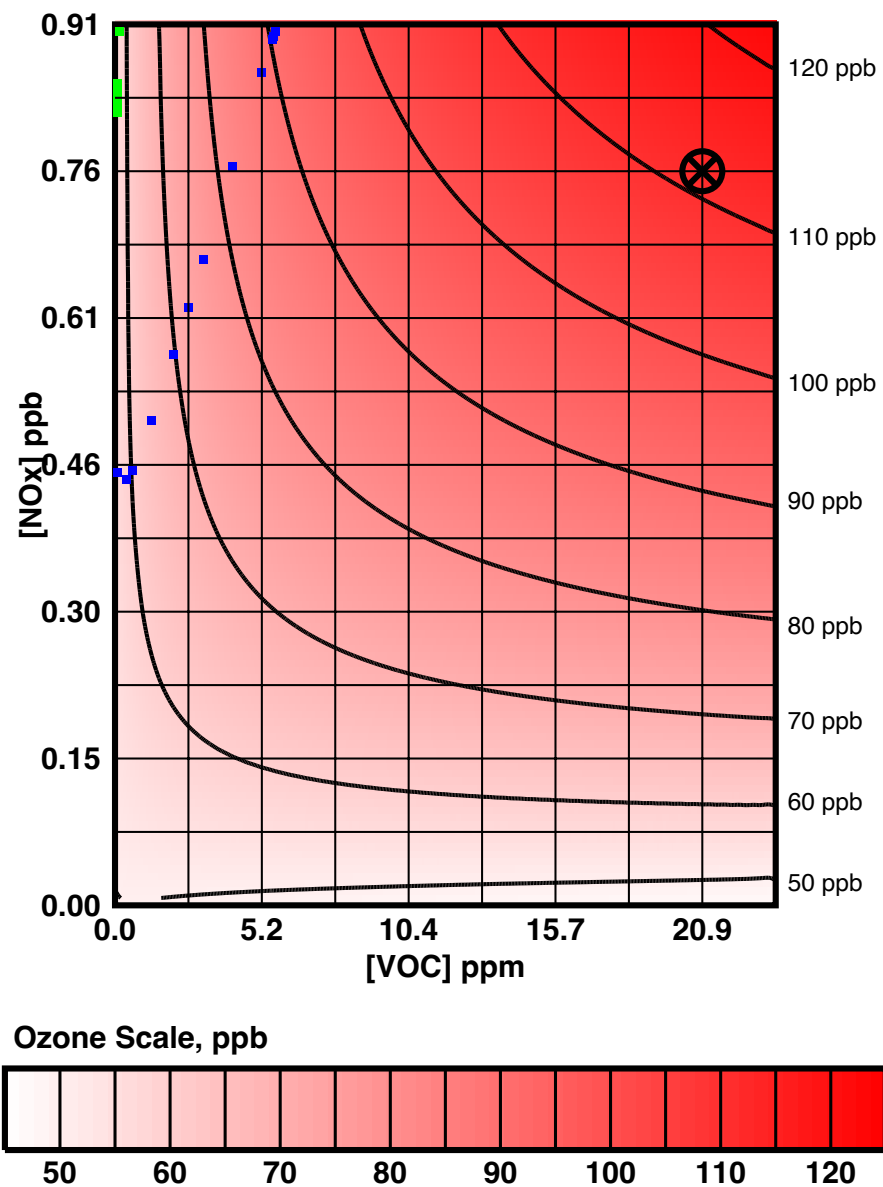


Figure S15. Model F17a, 2017-02-06.

F20a 2020-02-06

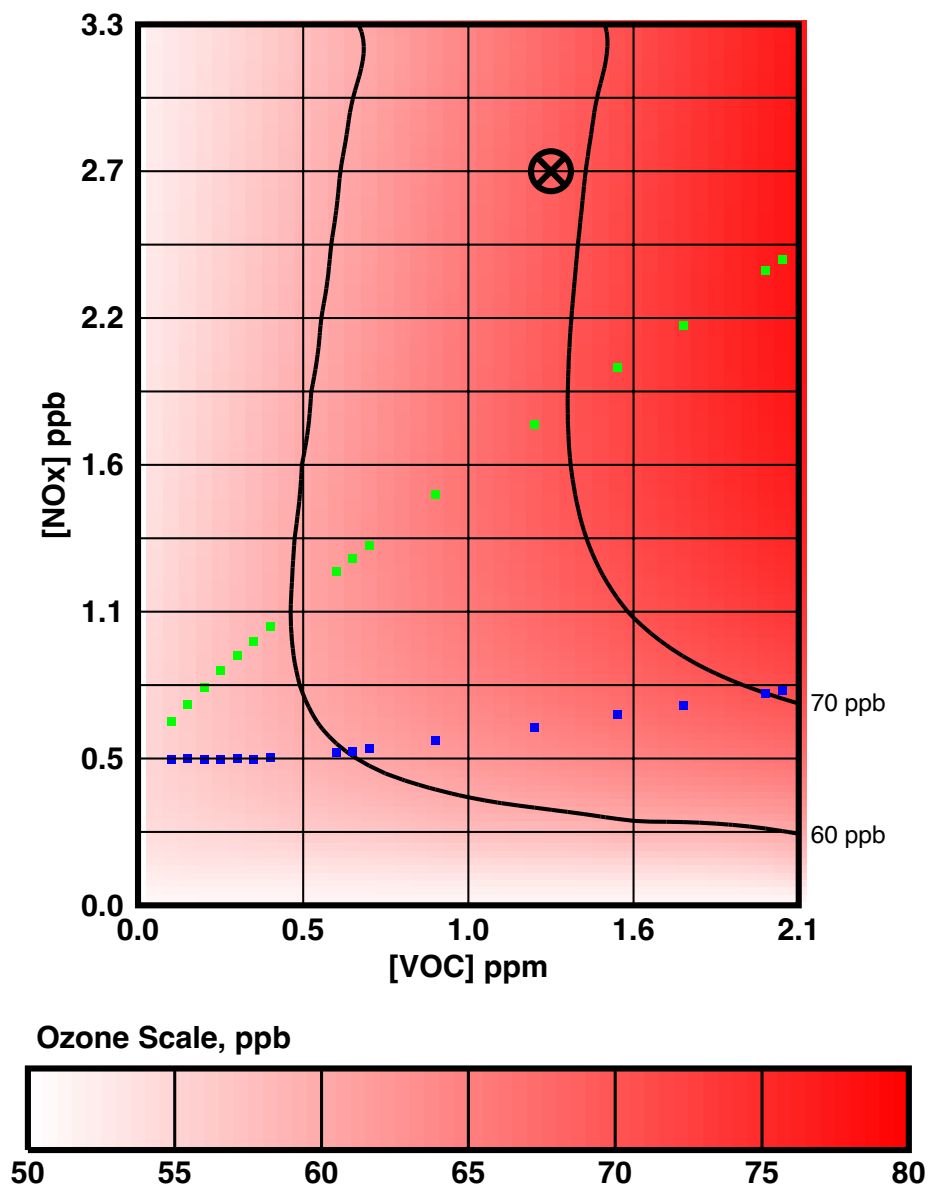


Figure S16. Model F20a, 2020-02-06.

F14a 2014-02-08

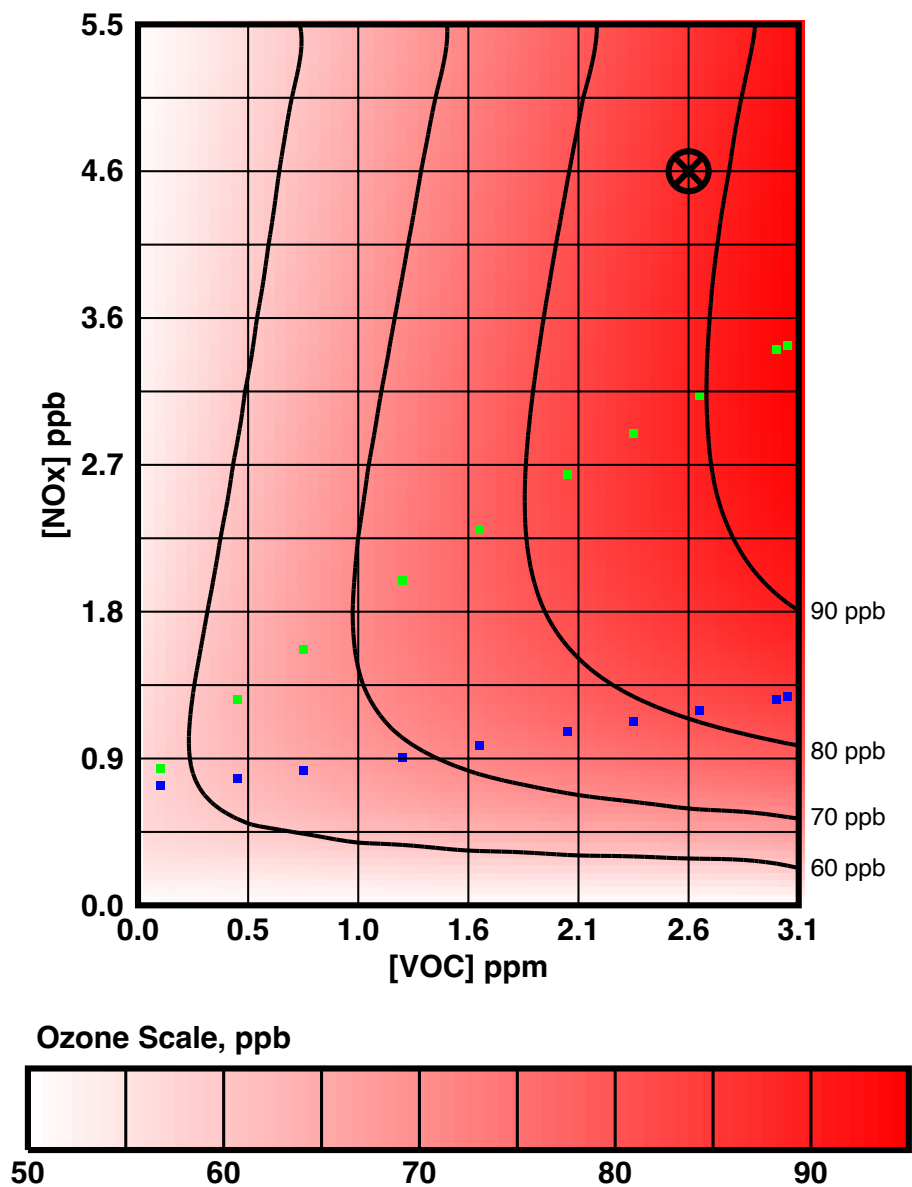


Figure S17. Model F14a, 2014-02-08.

F16a 2016-02-12

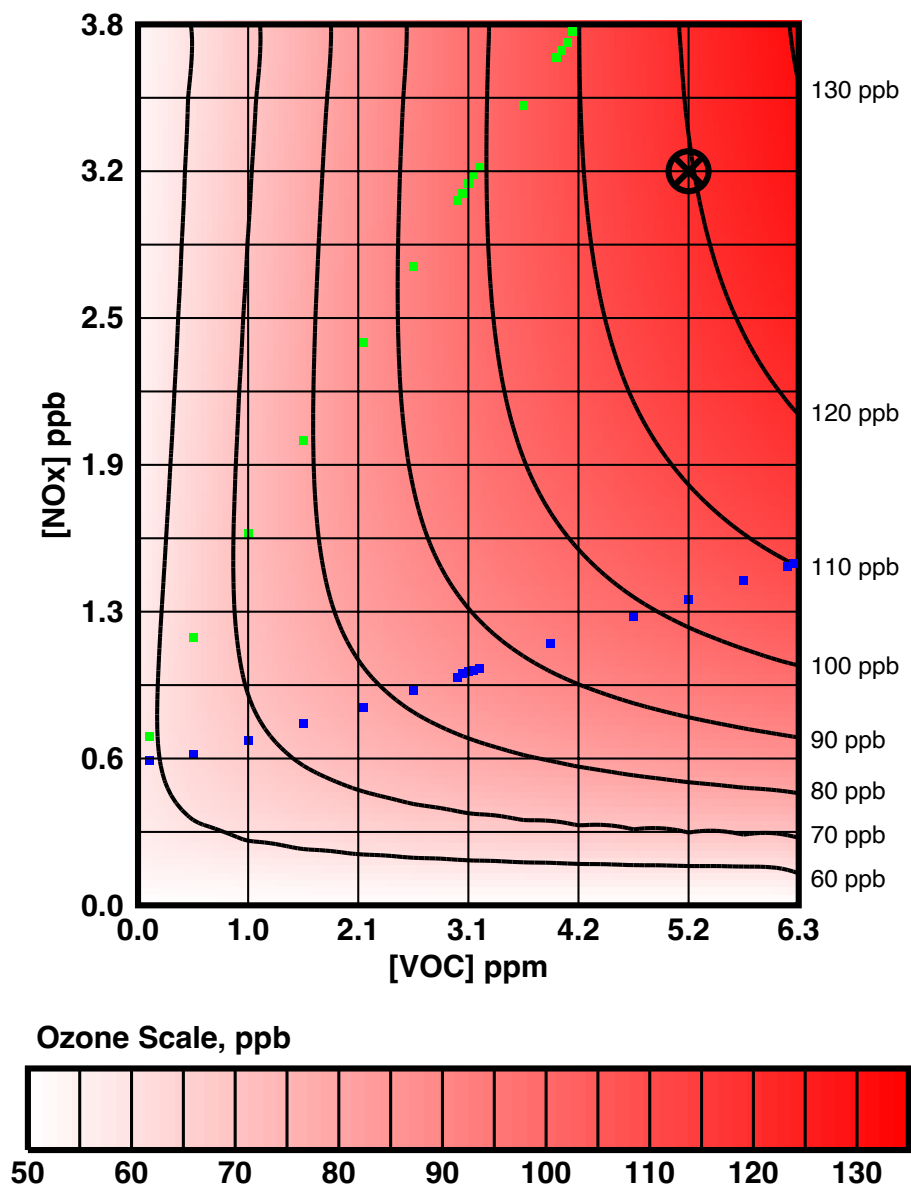


Figure S18. Model F16a, 2016-02-12.

F19b 2019-02-14

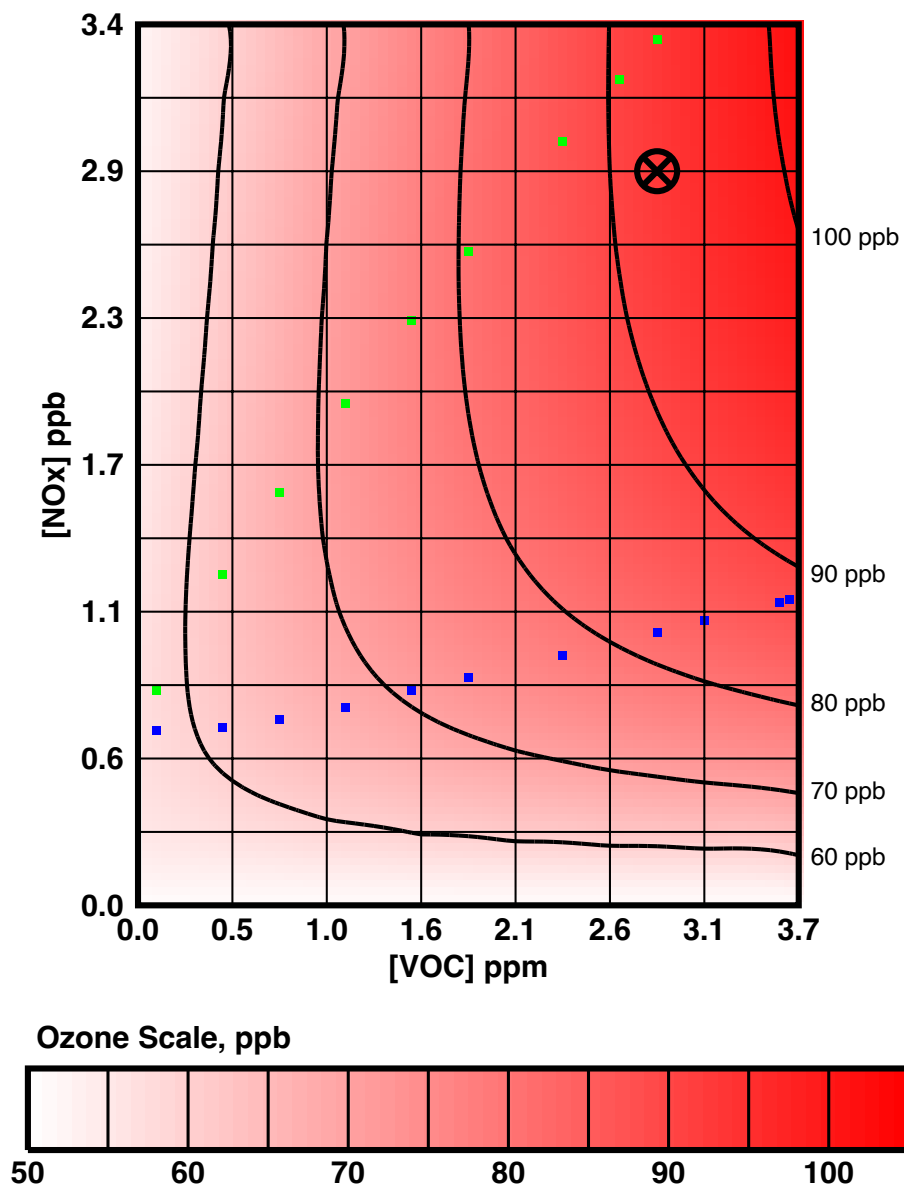


Figure S19. Model F19b, 2019-02-14.

F13b 2013-02-17

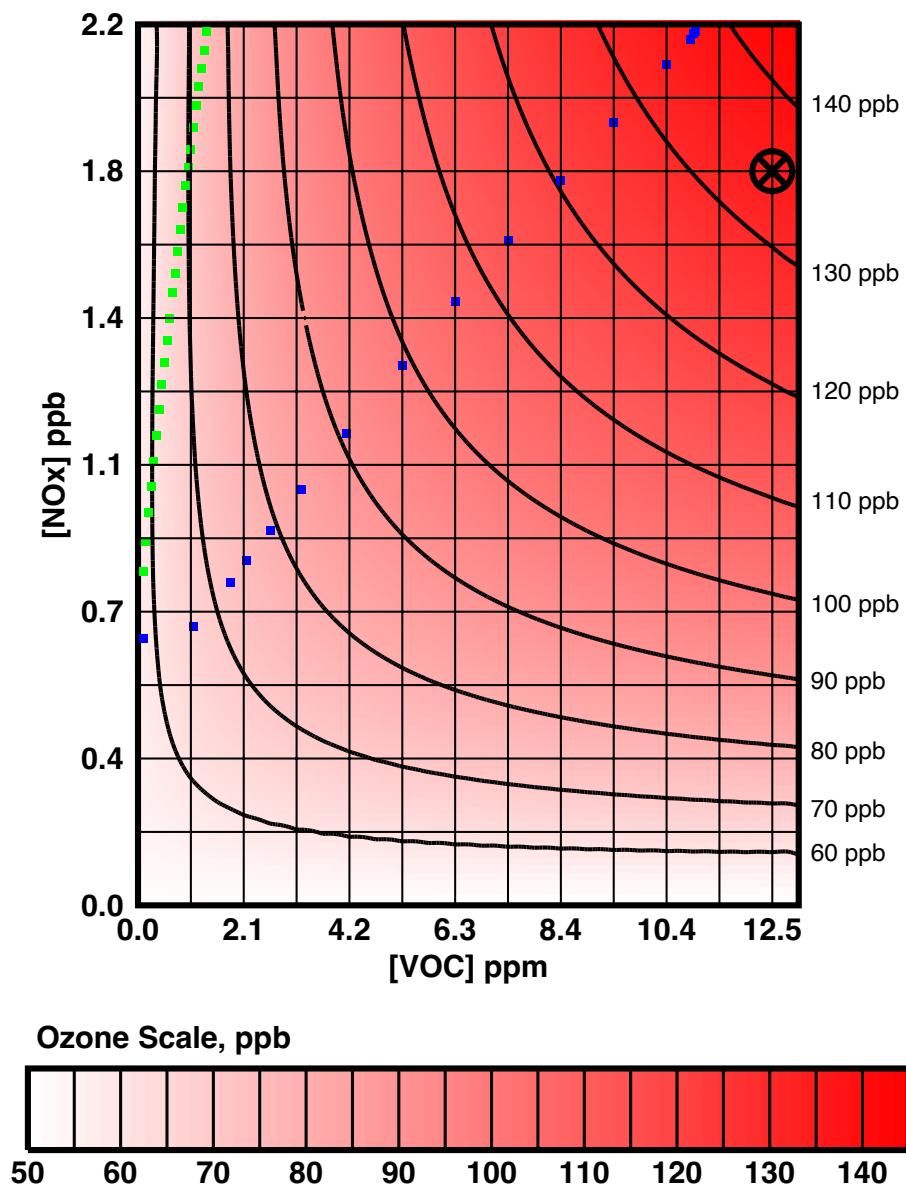


Figure S20. Model F13b, 2013-02-17.

F13c 2013-02-21

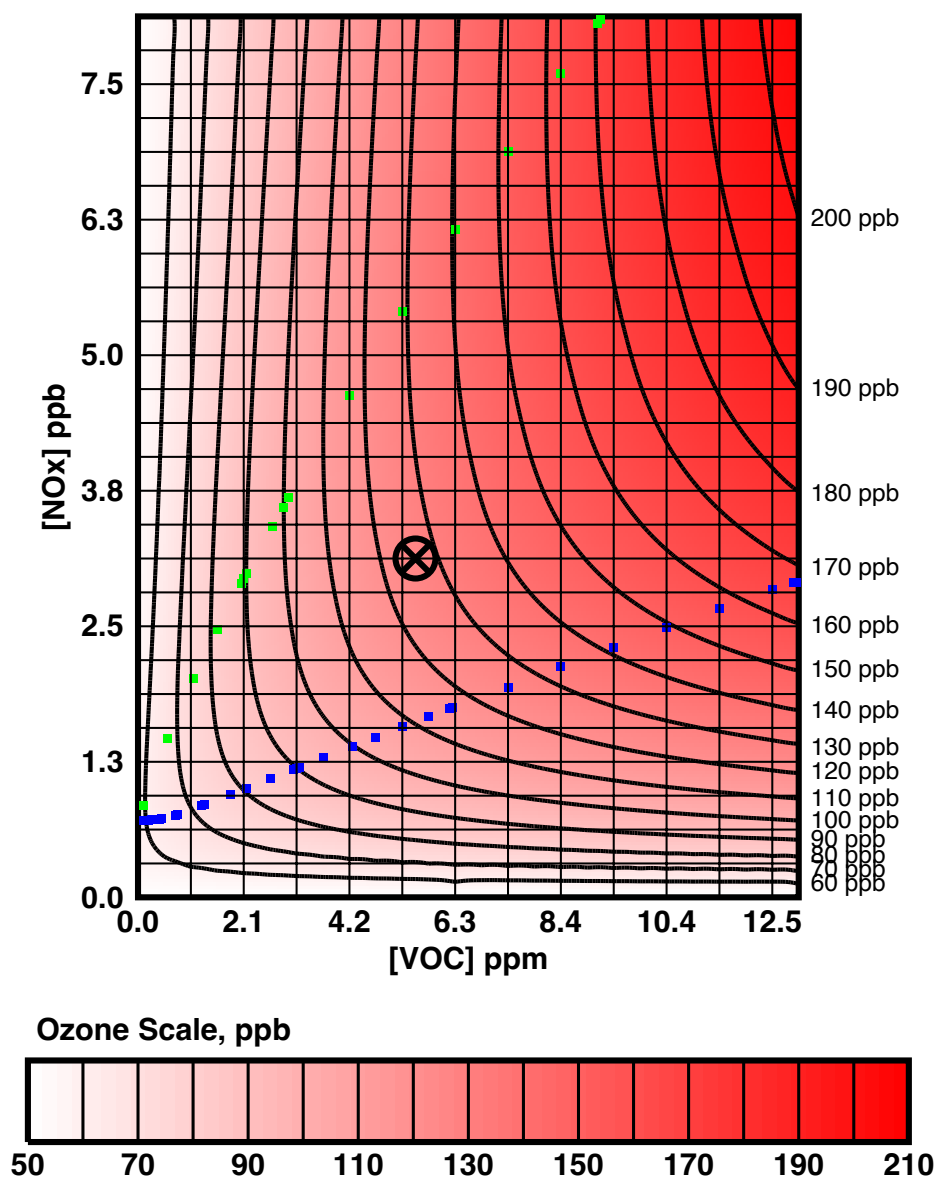


Figure S21. Model F13c, 2013-02-21.

F19c 2019-02-27

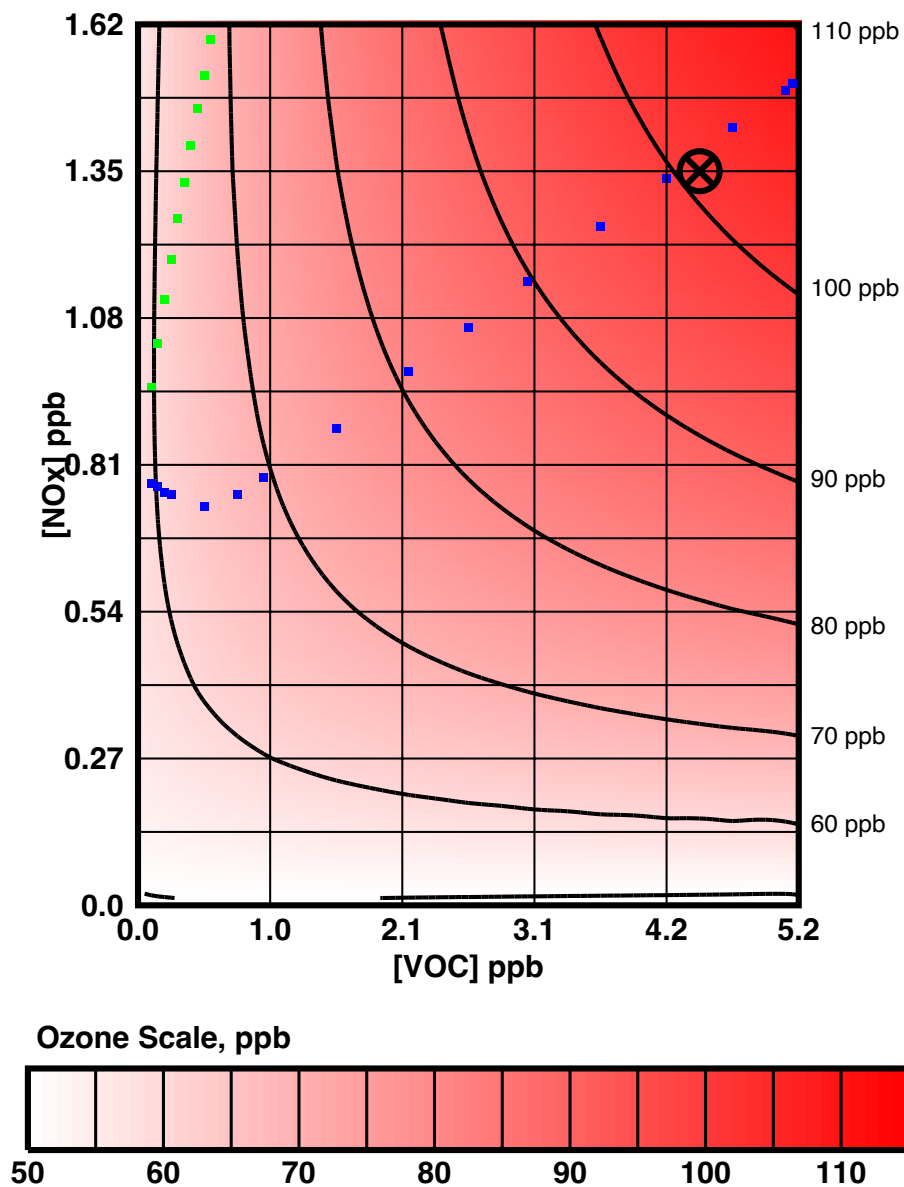


Figure S22. Model F19c, 2019-02-27.

M13a 2013-03-03

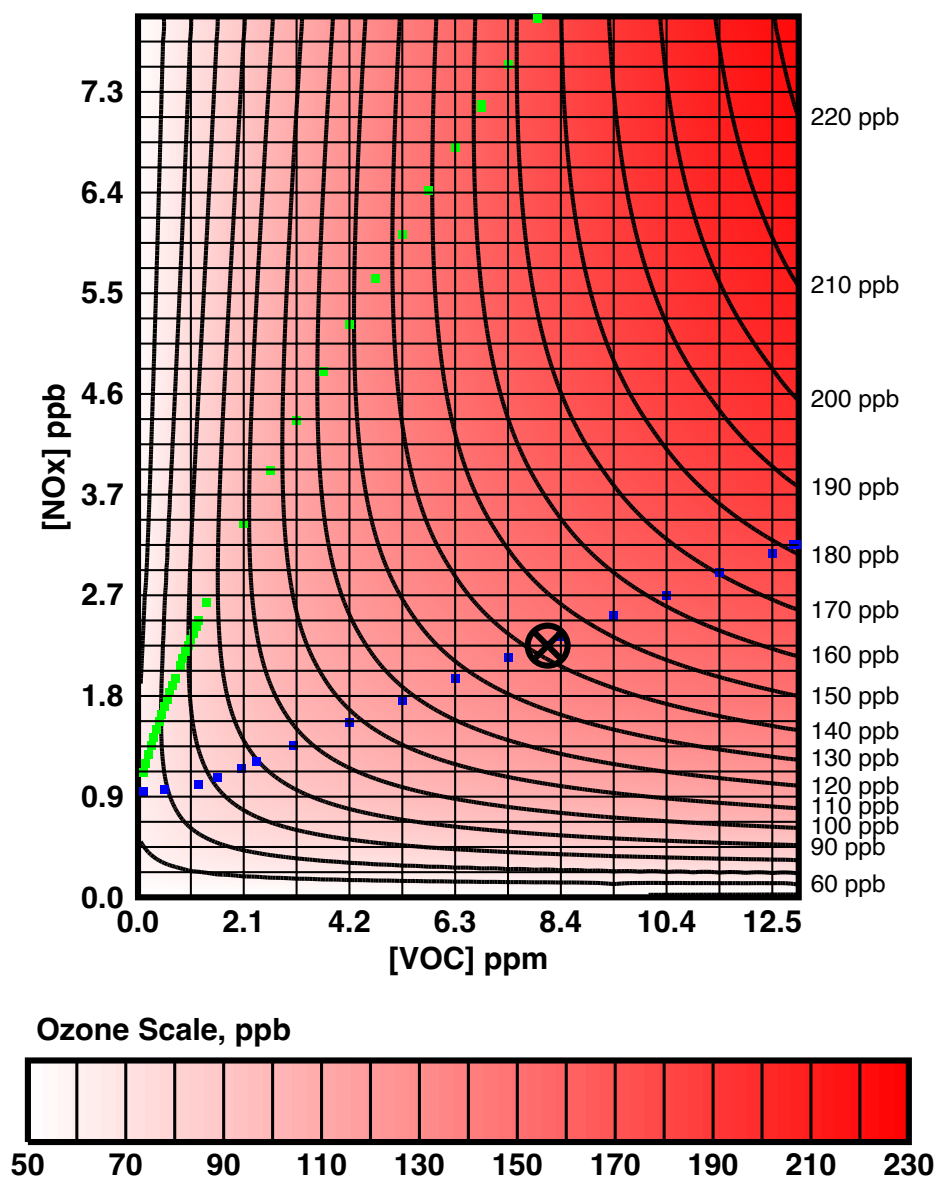


Figure S23. Model M13a, 2013-03-03.

M19a 2019-03-06

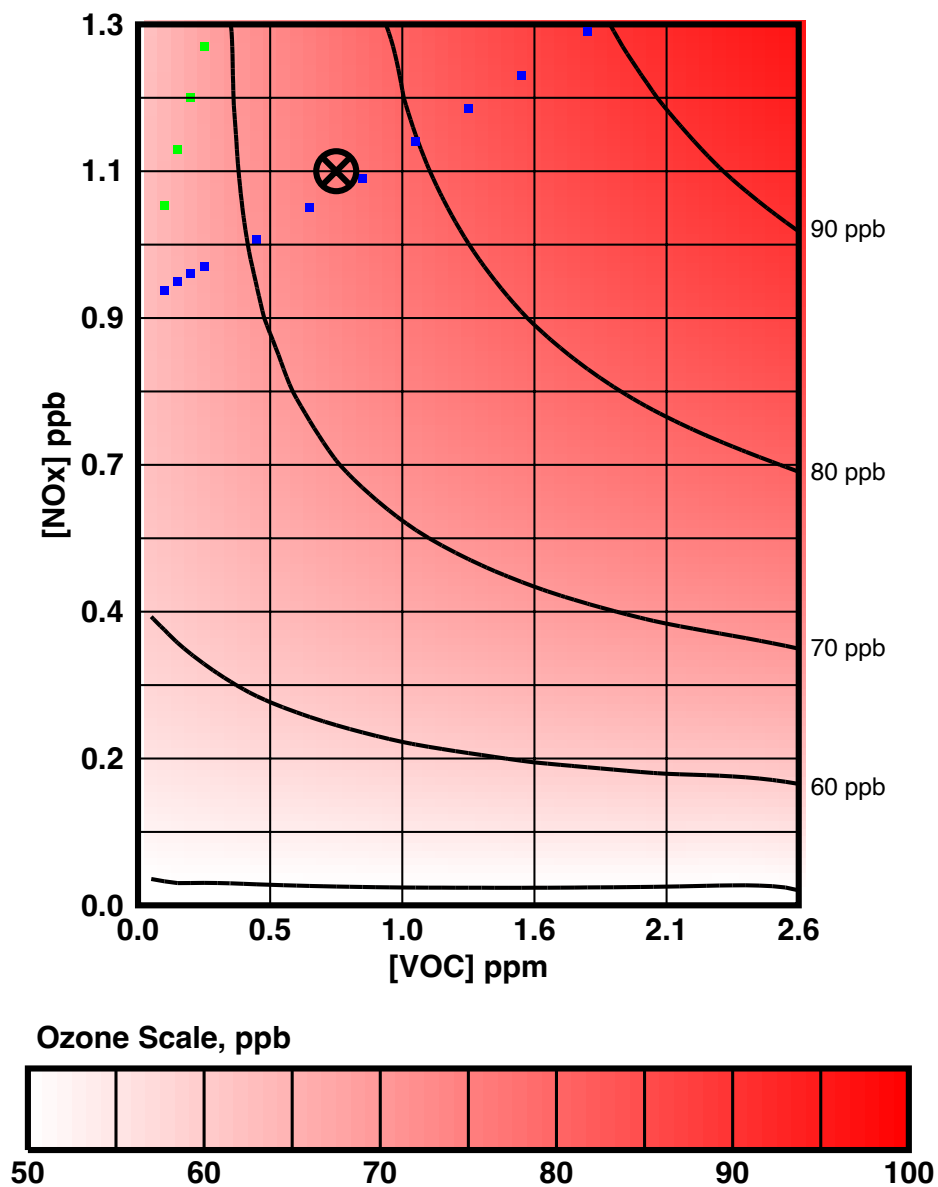


Figure S24. Model M19a, 2019-03-06.

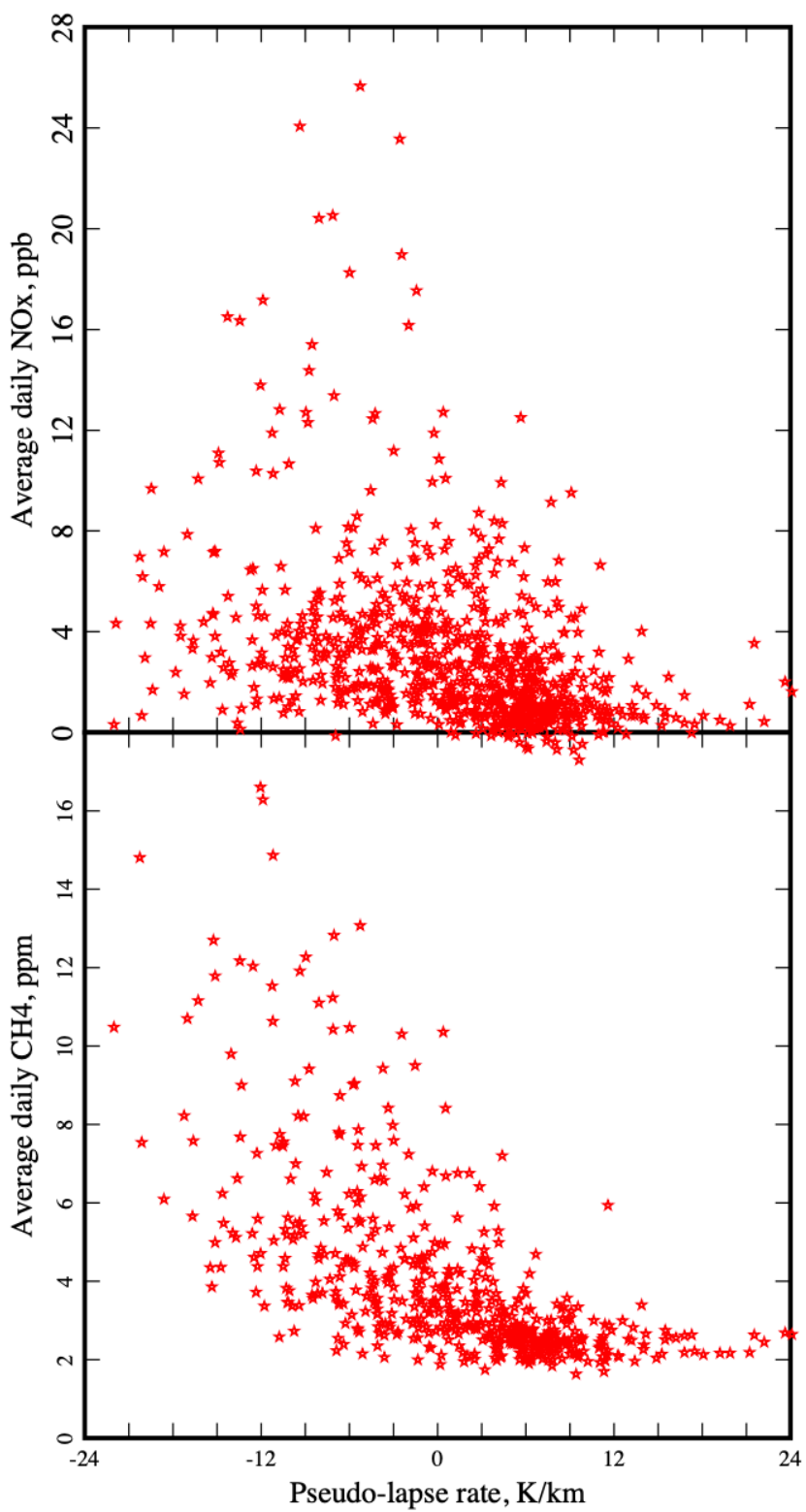


Figure S25. Correlations between NO_x and methane concentrations and the pseudo-lapse rate Ψ . Each symbol represents a daily average.

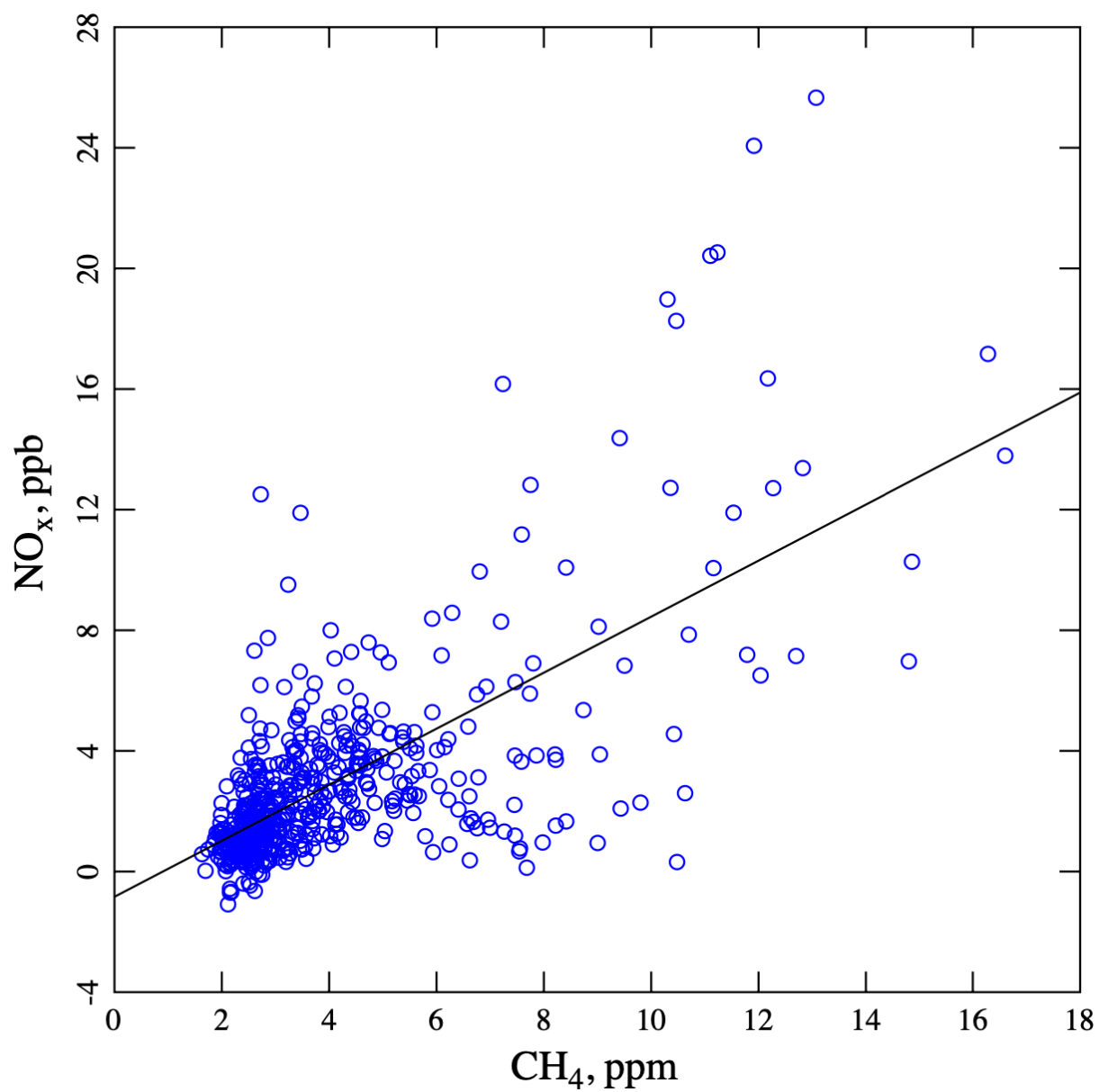


Figure S26. Correlations between NO_x and methane concentrations. Each symbol represents a pair of daily averages.